Surgery 165 (2019) 431–437

Contents lists available at ScienceDirect

Surgery

journal homepage: www.elsevier.com/locate/surg

Heterogeneous and low-intensity parathyroid autofluorescence: Patterns suggesting hyperfunction at parathyroid exploration

Emin Kose, MD, Bora Kahramangil, MD, Husnu Aydin, MD, Mustafa Donmez, MD, Eren Berber, MD*

Department of Endocrine Surgery, Cleveland Clinic, Cleveland, OH

ARTICLE INFO

Article history:
Accepted 7 August 2018
Available online 28 September 2018

ABSTRACT

Background: Although parathyroid glands have been found to exhibit autofluorescence with near-infrared fluorescence imaging, it is unknown if autofluorescence characteristics vary between hyperfunctioning and normofunctioning glands. The hypothesis was that pattern of autofluorescence exhibited by hyperfunctioning versus normofunctioning parathyroid glands would be different.

Methods: This is an Institutional Review Board–approved, prospective clinical study. Patients underwent bilateral neck exploration for primary hyperparathyroidism, during which autofluorescence from each gland was assessed with near-infrared fluorescence imaging. Pattern and intensity of autofluorescence between hyperfunctioning and normofunctioning parathyroid glands were compared.

Results: Overall, 199 parathyroid glands were identified in 50 patients (single gland disease, $n = 31$; multigland disease, $n = 19$). Autofluorescence was detected from 96% ($n = 192$) of parathyroid glands, all of which exhibited a higher intensity autofluorescence than the background tissues. Parathyroid gland location was revealed by near-infrared fluorescence imaging before dissection in 26% ($n = 52$). A total of 77 glands that were large or firm were excised and 122 were preserved because of normal appearance. Hyperfunctioning parathyroid glands had a lower mean normalized autofluorescence intensity than normofunctioning parathyroid glands (1.8, and 2.6, respectively, $P < .001$). Moreover, hyperfunctioning parathyroid glands more often exhibited a heterogeneous pattern of autofluorescence (75% and 5%, respectively, $P < .001$). On multivariate analysis, only parathyroid gland hyperfunction correlated with normalized autofluorescence intensity. On receiver operative characteristic curve, optimal cutoff of normalized autofluorescence intensity to differentiate hyperfunctioning from normofunctioning parathyroid glands was 2.0.

Conclusion: Our results indicate that hyperfunctioning and normofunctioning parathyroid glands exhibit different patterns of autofluorescence in hyperparathyroidism. Given these findings, autofluorescence pattern could be implemented as another adjunctive parameter for gland assessment during parathyroid exploration.

Introduction

Primary hyperparathyroidism (hyperparathyroidism) has a prevalence of 15.7 per 100,000 in the US population[1] and if untreated can cause serious complications, including nephrolithiasis, chronic kidney disease, and osteoporosis.[2] In eligible patients, surgery is the standard of care.[3] Nevertheless, intraoperative identification and assessment of the parathyroid glands (PGs) can be challenging even for experienced surgeons. Neck ultrasound and sestamibi scans are the 2 most commonly used localizing studies, accuracies of which range between 59% and 89% and 54% and 88%, respectively.[4] Despite the advances in these imaging modalities, the success of parathyroid surgery significantly depends on surgeon experience and has been reported to range from 91% to 100%.[5,6] The challenges with parathyroid localization and the importance of surgeon experience for a successful parathyroid surgery led to the famous quote by the interventional radiologist John L. Doppman: "In my opinion, the only localizing study indicated in a patient with untreated hyperparathyroidism is to localize an experienced parathyroid surgeon."[7]

Over the years, several imaging modalities have been proposed to localize PGs intraoperatively, including the use of aminolevulinic acid,[8] methylene blue,[9] a handheld gamma probe,[10] and most recently indocyanine green fluorescence.[11] However, these modalities could not consistently identify PGs and were associated with

* Reprint requests: Eren Berber, MD, 9500 Euclid Ave/F20, Cleveland, OH 44195.
E-mail address: berbere@ccf.org (E. Berber).

https://doi.org/10.1016/j.surg.2018.08.006
0039-6060/

adverse effects, such as injection-related complications, allergy, radiation exposure, and photosensitivity.[12] Furthermore, none of them predicted parathyroid function.[13]

Recently a novel method of identification that relies on the detection of autofluorescence from PGs using near-infrared fluorescence imaging (NIFI) has become available.[14] Initial reports have found up to 98% detection rates of PGs using this technique.[15] More recently it has also been suggested that rates of postoperative hypocalcemia after total thyroidectomy may be decreased with the use of this technology.[16] Despite many authors reporting the ability to detect autofluorescence from PGs intraoperatively,[15,17] whether this technology could be used to differentiate between hyperfunctioning and normofunctioning PGs has never been studied. Naturally a modality that could differentiate between hyperfunctioning and normofunctioning PGs would be very useful during parathyroid exploration. Therefore it is crucial to investigate this technology for a potential use in this regard. Our hypothesis was that the pattern of autofluorescence exhibited by hyperfunctioning versus normofunctioning PGs could be different. The aim of this study was to define these differences in autofluorescence patterns during parathyroid exploration for hyperparathyroidism.

Materials and methods

Study design

This was a prospective clinical study approved by the Institutional Review Board at the Cleveland Clinic. All study patients underwent bilateral neck exploration for hyperparathyroidism using autofluorescence imaging by a single surgeon (E.B.) between July 2016 and February 2018. Patients undergoing reoperative surgery were excluded.

The autofluorescence patterns between hyperfunctioning and normofunctioning PGs have never been compared before. Therefore an arbitrary number of 50 patients was decided for sample size.

Operative technique

We routinely perform a bilateral neck exploration assessing all 4 PGs at the Cleveland Clinic and have described the technique before.[4] All patients preoperative surgeon-performed neck ultrasound and all but 2 patients underwent sestamibi-iodine subtraction scans with single-photon emission computed tomography. In patients with positive localization studies, the initial dissection was performed for the localized gland. An intact parathyroid hormone (PTH) level was drawn from an anterior jugular vein before and 10 minutes after the excision of the preoperatively localized PG. While awaiting the results, other PGs were explored. Each identified PG gland was measured and palpated. All PGs that were larger than $5 \times 3 \times 1$ mm or were firm were excised.[18] In case of multigland disease, a 10-minute postexcision PTH level was also drawn after the removal of the last PG. In case of 4-gland hyperplasia, a 3.5 subtotal resection was performed with cryopreservation if all the glands were enlarged. In cases where 3 glands were enlarged but the last one found to be normal in size, a 3-gland excision was performed.

Parathyroid autofluorescence imaging was performed using a near-infrared camera (Fluobeam device, Fluoptics, Grenoble, France) held at the operative field from a 20-cm distance, with the operating room lights turned off. White light mode of the device was used to focus the camera on the operative field. Then the device was switched to NIFI mode to detect parathyroid autofluorescence. NIFI was initially performed after the strap muscles were dissected off the thyroid and central neck was exposed but before any explorative dissection. If PGs were not identified at this point, parathyroid exploration was commenced and NIFI repeated after dissection. Parathyroid autofluorescence was appreciated as a bright white spot on a dark background. Still and video images of each PG were taken. Each assessment took about a minute. Parathyroid tissue confirmation was obtained with frozen section for the removed glands and based on surgeon's judgment for the preserved glands. A candidate tissue was considered parathyroid tissue without further biopsy when harboring the following characteristic features: tan color, distinct shape and contour, and visible vasculature.

Autofluorescence intensity measurements

Autofluorescence intensities were measured using ImageJ software (National Institutes of Health, Bethesda, MD). For each PG, a representative photo was chosen for analysis to include the PG and the background tissues (muscle, trachea, or adipose tissue) in the same field. Using the software, the borders of the PG were marked, and mean black-and-white intensity (0–255) of the field was measured. A similarly sized area in the central neck soft tissue was marked and measured as the background. To decrease variability between different measurements, which may arise from minor differences in camera angle, camera distance, or residual background light in the operating room during each measurement, normalized autofluorescence intensities were calculated as normalized autofluorescence intensity = measured PG autofluorescence intensity / measured background intensity. The pattern of autofluorescence was scored as homogeneous when diffuse bright autofluorescence was detected from an index PG and heterogeneous when a mixture of bright and dim areas were appreciated. All data points were recorded intraoperatively into data collection forms.

Study variables

All data were collected prospectively and kept in an Institutional Review Board–approved database. Study variables included patient demographic characteristics; preoperative ultrasound and sestamibi scan findings; preoperative biochemical workup; NIFI findings (demonstration of autofluorescence, timing of PG identification [before dissection by NIFI or during dissection], PG size, PG autofluorescence intensity, background autofluorescence intensity, and autofluorescence pattern); PG functional status; and, for excised glands, final histopathologic findings and PG weight. Sestamibi and ultrasound scans were deemed positive if they suggested a functional or enlarged gland preoperatively and were deemed negative if no uptake or structure to suggest a functional or enlarged parathyroid were seen.

Functional status of individual PGs was determined as per the Miami criterion.[19] An index PG was scored as hyperfunctioning if at least a 50% drop in PTH levels was obtained after its excision compared with the pre-excision level. An index PG was scored as normofunctioning when the 50% drop did not occur. As per our institutional practice, if a PG appeared grossly abnormal on surgical exploration (enlarged or firm), it was excised even if a 50% drop was achieved previously after removal of another PG. Parathyroid cellularity was determined by pathologists who were blinded to the results of autofluorescence. A gland was deemed hypercellular based a combination of findings including increased number of parathyroid cells versus fat, abnormal architecture (follicular or trabecular), presence of solid areas, and homogenous cytomorphology (ie, all chief, clear, or oxyphilic cells).

The patients were followed with serum calcium, PTH, and phosphorus levels on postoperative days 1 and 14 and at 6 months postoperatively. Cure was defined as normocalcemia with normal PTH levels beyond 6 months in follow-up.

Table 1
Demographic and clinical details of the study patients.

Parameter	All patients (n = 50)
Age, y, mean (SD)	59.6 (12.4)
Sex, n (%)	
Male	8 (16)
Female	42 (84)
Body mass index, kg/m^2, mean (SD)	30.4 (6.9)
Preoperative localizing studies	
Sestamibi scan: positive/negative*	28/20
Ultrasound: positive/negative	29/21
Both sestamibi and ultrasound positive	21 (42)
Both sestamibi and ultrasound negative	13 (26)
Preoperative workup, median (range)	
Parathyroid hormone	93 (54–247)
Calcium	10.7 (9.1–12)
Phosphate	2.7 (1.7–4.6)
25-hydroxy-vitamin D	31.5 (13.1–63)
24 hour urinary calcium/creatinine	220.5 (42.6–392.7)
Lowest T-score on DEXA scan	−1.9 ([−4.1]–[−0.6])

*Includes patients who underwent sestamibi scan preoperatively (n = 48 patients).
DEXA, dual-energy x-ray absorptiometry; *SD,* standard deviation.

Statistical analysis

Statistical analysis was performed using JMP Version 13.1 (SAS Institute, Inc, Cary, NC). Demonstration of autofluorescence, timing of identification, size, cellularity, normalized autofluorescence intensity, and autofluorescence pattern were compared between hyperfunctioning and normofunctioning PGs. Simple linear regression was performed to identify the clinical parameters associated with normalized autofluorescence intensity. Parameters with a P value ≤.10 on univariate analysis were included in the multivariate model. All identified PGs were grouped as hyperfunctioning (includes excised PGs with ≥50% PTH drop postexcision) and normofunctioning (includes excised PGs with <50% PTH drop postexcision and PGs preserved because of normal morphologic features). Receiver operating characteristics curve was constructed to identify the most sensitive, most specific, and optimal cutoffs of normalized autofluorescence intensity to predict hyperfunction of an imaged gland.

Results

A total of 50 patients underwent bilateral neck exploration for hyperparathyroidism. A PG was localized successfully by preoperative ultrasound in 29 of 50 (58%), by sestamibi in 28 of 48 (58%), and by concordance of both studies in 21 patients. In 20 patients the sestamibi, in 21 patients the ultrasound, and in 13 patients both sestamibi and ultrasound were negative. Based on intraoperative findings, 31 patients were found to have a single adenoma, 11 patients double adenomas, and 8 patients 4-gland hyperplasia. In all patients but one, all 4 PGs could be identified. None of the patients had supernumerary PGs. Table 1 summarizes the demographic and clinical details. In all patients, intraoperative PTH levels dropped appropriately as per Miami criterion. Median follow-up was 7 months (range: 3–22 months). At the time of this writing, 37 patients were cured at 6-month bloodwork, whereas 13 patients had normalization of their serum calcium and PTH values on postoperative visits done at less than 6 months postoperatively.

Intraoperatively a total of 199 PGs were identified, 96% (n = 192) of which exhibited autofluorescence detected by NIFI. In all of these 192 PGs, measured autofluorescence intensity was greater than that of the background central neck tissues. Table 2 summarizes the details of autofluorescence imaging. Notably, the locations of 52 PGs (26%) were revealed by autofluorescence before dissection and visual identification. Of the 199 PGs identified, 77 were excised and 122 preserved (3 with partial resection as part of 4-gland hyperplasia). According to the Miami criterion, 65 of the excised PGs were hyperfunctioning (60 hypercellular and 5 normocellular on final pathologic examination) and 12 normofunctioning (6 hypercellular and 6 normocellular). Mean normalized autofluorescence intensity of the hyperfunctioning glands was lower than that of normofunctioning glands (1.8 vs. 2.6, P < .001). Furthermore, hyperfunctioning PGs more often displayed a heterogenous pattern of autofluorescence (75% vs 5%, P < .001; Figs 1, 2, and 3).

On univariate analysis, PG size, detection on sestamibi scan, hypercellularity, and hyperfunction indicated correlation with normalized autofluorescence intensity. In the multivariate model, only hyperfunction remained as an independent predictor (correlation coefficient −0.66, 95% confidence interval −1.19 to −0.13; P = .02; Table 3). On the receiver operating characteristic curve, the 100% sensitive, 100% specific, and optimal cutoffs of normalized autofluorescence intensity to differentiate hyperfunctioning from normofunctioning PGs were 3.8, 1.1, and 2.0, respectively (Fig 4).

When parathyroid glands involved in single adenomas versus multigland disease were compared, it was found that normalized autofluorescence intensity was 1.8 vs 2.0 (P = .12), whereas the rate of heterogeneous intensity was 81% vs 54% (P = .02), respectively.

Discussion

To our knowledge this is the first study in the literature suggesting that different patterns of autofluorescence are exhibited by hyperfunctioning versus normofunctioning PGs in hyperparathy-

Table 2
Autofluorescence imaging findings of parathyroid glands.

Parameter	Hyperfunctioning (n = 65)	Normofunctioning (n = 134)	P
No. of PGs demonstrating autofluorescence, n (%)	63 (97)	129 (96)	.81
First method of identification, n (%)			.73
Before dissection by NIFI	16 (25)	36 (27)	
After dissection	49 (75)	98 (73)	
Largest diameter, mm, mean (SD)	14.0 (8.6)	6.1 (2.5)	**<.001**
Weight, g, mean (SD)*	0.3 (0.3)	0.1 (0.1)	**.01**
Normalized autofluorescence intensity, mean (SD)†	1.8 (0.63)	2.6 (1.0)	**<.001**
Autofluorescence pattern†			**<.001**
Heterogeneous, n (%)	47/63 (75)	7/129 (5)	
Homogeneous, n (%)	16/63 (25)	122/129 (95)	
Pathology			**<.001**
Hypercellular	60 (92)	6 (4)	
Normocellular	5 (8)	128 (96)	

* Includes only resected parathyroid glands (n = 77).
† Includes only parathyroid glands that exhibited autofluorescence on near-infrared excitation (n = 192). *SD,* standard deviation.

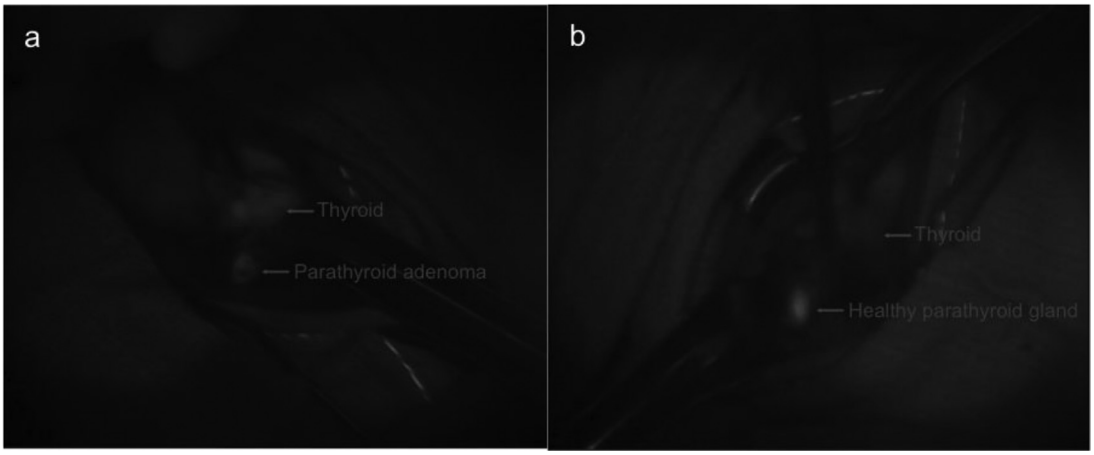

Figure 1. Intraoperative photos showing a heterogeneous, lower intensity autofluorescence detected from an excised parathyroid adenoma (A) versus a preserved, suppressed parathyroid gland (B). The normalized autofluorescence intensities of these glands were 2.0 and 5.1, respectively. The patient's parathyroid hormone levels normalized postoperatively.

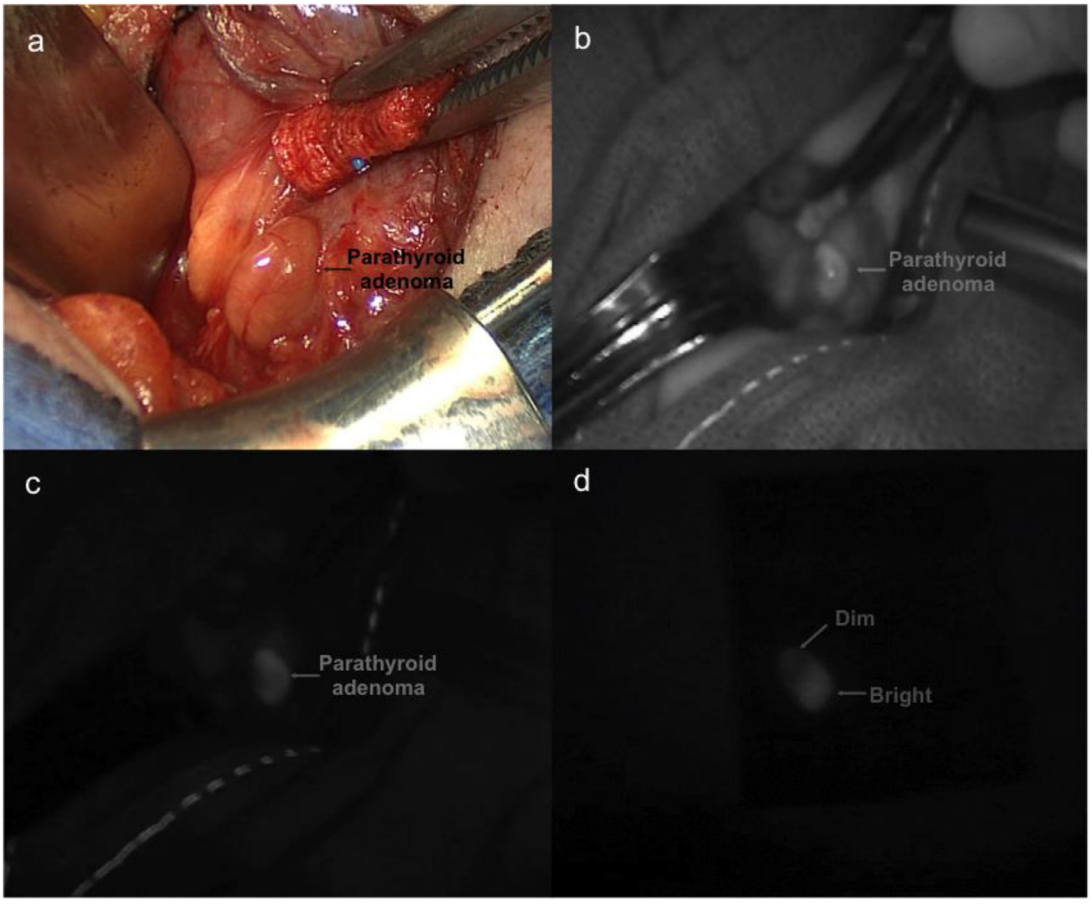

Figure 2. Intraoperative captures of a parathyroid adenoma. On exploration (A), the gland was larger and firmer than normal. After turning down the operating room lights, the gland was identified using the white-light mode (B) of the near-infrared fluorescence system followed by autofluorescence imaging (C). The heterogeneous autofluorescence detected from this gland was noted to persist ex vivo after excision (D).

roidism. Despite the previous studies reporting the use of parathyroid autofluorescence imaging to identify PGs during thyroidectomy and parathyroidectomy,[15,17] its use to predict parathyroid function has not been reported before. We have found that hyperfunctioning glands have heterogeneous and low-intensity autofluorescence compared with normofunctioning glands. Of note, our results are in opposition to an earlier study that reported higher autofluorescence intensity measurements from hypercellular compared with normal glands in 7 patients with hyperparathyroidism.[20] In light of the present findings, we believe that autofluorescence pattern detected from each PG could be an adjunctive parameter incorporated into surgical decision-making. The finding of a bright, homogeneous autofluorescence from a given PG could decrease the suspicion that it is abnormal. Conversely, detection of low intensity, heterogeneous autofluorescence would suggest that the gland is likely hyperfunctioning. In essence, this concept could

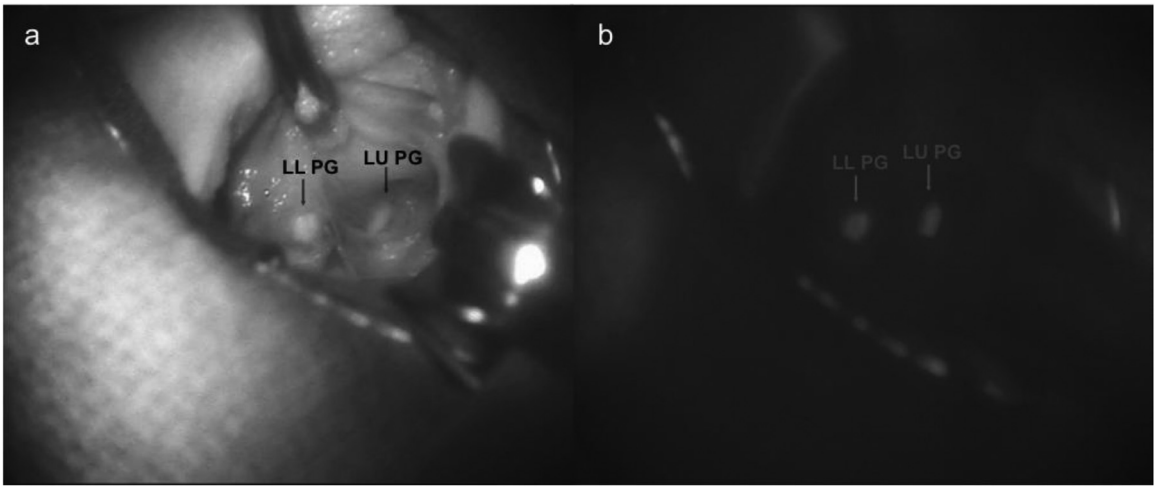

Figure 3. Intraoperative photos of 2 suppressed parathyroid glands. After localization in white-light mode (A), autofluorescence imaging (B) was performed. Bright and homogeneous autofluorescence was detected from both glands. *LL*, left lower; *LU*, left upper; *PG*, parathyroid gland.

Table 3
Simple linear regression for predictors of normalized autofluorescence intensity.

	Univariate			Multivariate		
Parameter	CC	95% CI	P	CC	95% CI	P
Parathyroid gland size (mm)	−0.04	−0.07 to −0.02	**<.001**	−0.01	−0.04 to 0.01	.36
Preoperative Ca (mg/dL)	−0.04	−0.28 to 0.19	.7	—	—	—
24-hour urinary calcium (mg/24 h)	−0.0001	−0.002 to 0.001	.89	—	—	—
Preoperative parathyroid hormone (pg/mL)	−0.002	−0.005 to 0.0009	.18	—	—	—
25-hydroxy–vitamin D (ng/mL)	−0.005	−0.01 to 0.006		—	—	—
Body mass index (kg/m^2)	−0.003	−0.02 to 0.02	.75	—	—	—
Hypercellularity	−0.73	−1.00 to −0.46)	**<.001**	−0.1	−0.65 to 0.44	.71
Detection on sestamibi scan	−0.6	−0.97 to −0.23	**.002**	−0.06	−0.48 to 0.35	.76
Hyperfunction	−0.85	−1.11 to −0.58	**<.001**	−0.66	−1.19 to −0.13	**.02**

CC, correlation coefficient; *CI*, confidence interval.

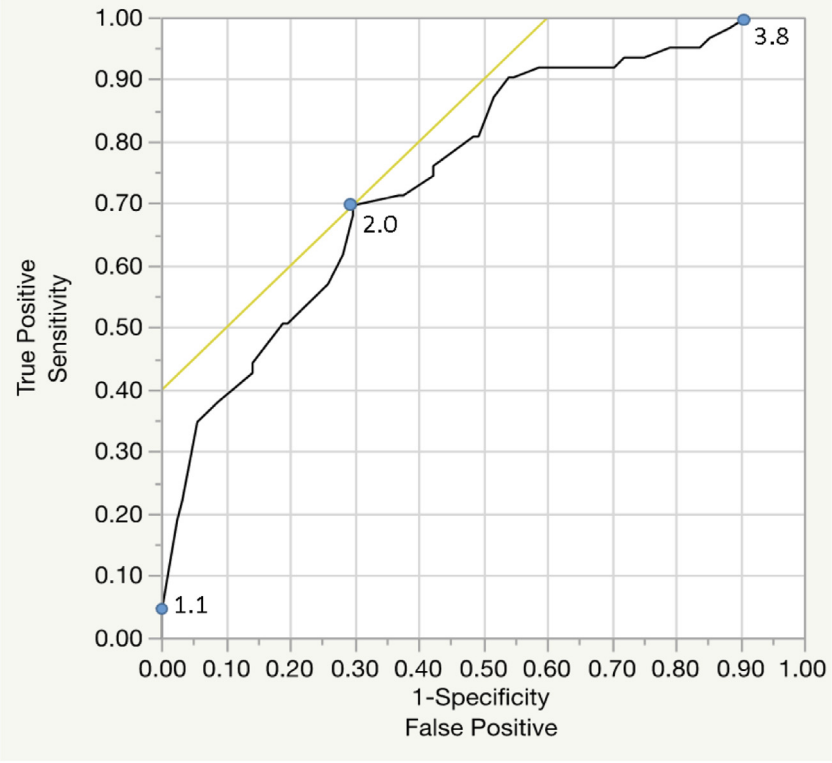

Figure 4. Receiver operating characteristics curve of normalized autofluorescence intensity in predicting hyperfunction. Area under curve: 0.78.

become analogous to a noninvasive alternative to frozen section to predict a given gland's pathologic status.

Intrigued by the differences in the patterns of autofluorescence exhibited by the hyperfunctioning and normofunctioning PGs, our pathologists have identified a number of changes in the glands with low-intensity, heterogeneous autofluorescence, including increased cellularity, patchy areas of fibrosis, oxyphilic cell clusters, and areas of hematoma. We hypothesize that pathologic PGs may lose the ability to emit strong, homogeneous autofluorescence. However, the description of the correlation between histopathologic changes and autofluorescence patterns was beyond the scope of this manuscript. Although some studies have suggested that calcium receptor protein, which is present in high concentrations in the parathyroid chief cells, may be responsible for parathyroid autofluorescence,[21,22] the exact chemical nature of the endogenous parathyroid fluorophore remains unknown.

According to the 2016 American Association of Endocrine Surgeons guidelines, both focal and bilateral neck explorations are considered appropriate operations with high cure rates.[3] The relatively high (38%) rate of multigland disease is inherently related to the principles of bilateral exploration, which rely on the removal of any large or firm glands, irrespective of the intraoperative PTH values. Nevertheless, because of our intraoperative PTH protocol, we were able to categorize each gland as hyper- or normofunctioning and perform statistical analyses accordingly. Notably, the low sestamibi scan sensitivity of 58% in the present series likely was due to referral practices. We oftentimes serve as a referral center for patients with negative localizing studies in community settings.

Overall, we believe that this technology will be of higher use to inexperienced surgeons in the identification and assessment of PGs during. The price of the imaging system in the US market is unknown at this time. The system can be set up in a few minutes by the operating room personnel and controlled with a few buttons. The only additional requirement is a sterile cover. We have not experienced any malfunctions or breakdowns with this system to date.

Notably, in the present study, 26% of PGs were detected by NIFI before visual identification by the surgeon during bilateral neck exploration for hyperparathyroidism. Although these glands would likely later be identified during the procedure, autofluorescence imaging facilitated their early detection, possibly shortening the procedure. In the present series, no intrathyroidal PGs were detected. In our larger experience with NIFI, including thyroidectomies, we have found that only intracapsular, intrathyroidal PGs could be detected using NIFI. More deeply located intrathyroidal PGs could not be visualized with this technique because of the limited depth of penetration of near-infrared light.

There are some limitations to this technology. First, the hand piece is larger than the small incisions used for parathyroid exploration. This makes focusing of the camera on the surgical field challenging. We believe that a learning curve of 15 to 20 cases is necessary to optimally use this technology. In addition, the numeric values related to autofluorescence in this study were generated using a third-party software. Finally, for autofluorescence imaging, the current system requires the operating room lights to be turned off. Although there is a built-in white light mode to help orient the camera to the field, the current system needs switching back and forth between autofluorescence and white light modes. New-generation systems should use smaller camera pieces, built-in signal quantification, and fused autofluorescence and white light images to overcome these issues.

Previous studies have reported on the feasibility of detecting parathyroid autofluorescence using NIFI. In 2011 the Vanderbilt group described for the first time the intraoperative use of near-infrared spectroscopy to detect parathyroid autofluorescence.[14] In their largest clinical study to date, this group could correctly identify 97% of 264 PGs using this technique.[17] Using the system described in the present study, Falco et al[20] reported in 2016 that mean fluorescent intensities of PG, thyroid gland, and background soft tissues were different at 40.6, 31.8, and 16.6, respectively. The same group later reported that an increased number of PGs could be identified intraoperatively with the incorporation of NIFI (mean number of PGs: 3.7 and 2.5, with and without NIFI, respectively).[23] In the largest multicenter clinical study to date evaluating NIFI of parathyroid autofluorescence, we previously reported that autofluorescence imaging could correctly identify 98% of PGs intraoperatively. Furthermore, in 37% to 67% of cases, the location of the PGs were revealed by NIFI before visual identification by the operating surgeon.[15] Recently, Benmiloud et al[16] looked at the impact of parathyroid autofluorescence imaging on hypocalcemia rates after total thyroidectomy and noted a decrease from 20.9% to 5.2% with the incorporation of NIFI.

In addition to the differences detected with autofluorescence between hyperfunctioning and normofunctioning PGs, another finding of the present study was that glands involved in single adenomas versus multigland disease more often exhibited a heterogenous pattern of intensity. The significance of this observation will be investigated in future studies.

In conclusion, this study found that hyperfunctioning and normofunctioning PGs in hyperparathyroidism exhibit different patterns of autofluorescence on excitation with NIFI. Given these findings, autofluorescence pattern could be a new adjunctive parameter for the intraoperative assessment of PGs. In addition to the advances in preoperative localizing studies and intraoperative PTH and development of focal exploration techniques in recent decades, this technology might represent a new breakthrough in parathyroid surgery.

References

1. Wermers RA, Khosla S, Atkinson EJ, Achenbach SJ, Oberg AL, Grant CS, et al. Incidence of primary hyperparathyroidism in Rochester, Minnesota, 1993-2001: an update on the changing epidemiology of the disease. *J Bone Miner Res*. 2006;21:171–177.
2. Bilezikian JP, Brandi ML, Rubin M, Silverberg SJ. Primary hyperparathyroidism: new concepts in clinical, densitometric and biochemical features. *J Intern Med*. 2005;257:6–17.
3. Wilhelm SM, Wang TS, Ruan DT, Lee JA, Asa SL, Duh QY, et al. The American Association of Endocrine Surgeons guidelines for definitive management of primary hyperparathyroidism. *JAMA Surg*. 2016;151:959–968.
4. Siperstein A, Berber E, Barbosa GF, Tsinberg M, Greene AB, Mitchell J, et al. Predicting the success of limited exploration for primary hyperparathyroidism using ultrasound, sestamibi, and intraoperative parathyroid hormone: analysis of 1158 cases. *Ann Surg*. 2008;248:420–428.
5. Westerdahl J, Bergenfelz A. Unilateral versus bilateral neck exploration for primary hyperparathyroidism: five-year follow-up of a randomized controlled trial. *Ann Surg*. 2007;246:976–980 discussion 980.
6. Inabnet WB, Dakin GF, Haber RS, Rubino F, Diamond EJ, Gagner M. Targeted parathyroidectomy in the era of intraoperative parathormone monitoring. *World J Surg*. 2002;26:921–925.
7. Kunstman JW, Kirsch JD, Mahajan A, Udelsman R. Clinical review: parathyroid localization and implications for clinical management. *J Clin Endocrinol Metab*. 2013;98:902–912.
8. Prosst RL, Gahlen J, Schnuelle P, Post S, Willeke F. Fluorescence-guided minimally invasive parathyroidectomy: a novel surgical therapy for secondary hyperparathyroidism. *Am J Kidney Dis*. 2006;48:327–331.
9. Dudley NE. Methylene blue for rapid identification of the parathyroids. *Br Med J*. 1971;3:680–681.
10. Grubbs EG, Mittendorf EA, Perrier ND, Lee JE. Gamma probe identification of normal parathyroid glands during central neck surgery can facilitate parathyroid preservation. *Am J Surg*. 2008;196:931–935 discussion 935.
11. Zaidi N, Bucak E, Okoh A, Yazici P, Yigitbas H, Berber E. The utility of indocyanine green near infrared fluorescent imaging in the identification of parathyroid glands during surgery for primary hyperparathyroidism. *J Surg Oncol*. 2016;113:771–774.
12. Kahramangil B, Berber E. Comparison of indocyanine green fluorescence and parathyroid autofluorescence imaging in the identification of parathyroid glands during thyroidectomy. *Gland Surg*. 2017;6:644–648.
13. Kahramangil B, Berber E. The use of near-infrared fluorescence imaging in endocrine surgical procedures. *J Surg Oncol*. 2017;115:848–855.
14. Paras C, Keller M, White L, Phay J, Mahadevan-Jansen A. Near-infrared autofluorescence for the detection of parathyroid glands. *J Biomed Opt*. 2011;16:067012.

15. Kahramangil B, Dip F, Benmiloud F, Falco J, de La Fuente M, Verna S, et al. Detection of parathyroid autofluorescence using near-infrared imaging: a multicenter analysis of concordance between different surgeons. *Ann Surg Oncol*. 2018;25:957–962.
16. Benmiloud F, Rebaudet S, Varoquaux A, Penaranda G, Bannier M, Denizot A. Impact of autofluorescence-based identification of parathyroids during total thyroidectomy on postoperative hypocalcemia: a before and after controlled study. *Surgery*. 2018;163:23–30.
17. McWade MA, Sanders ME, Broome JT, Solorzano CC, Mahadevan-Jansen A. Establishing the clinical utility of autofluorescence spectroscopy for parathyroid detection. *Surgery*. 2016;159:193–202.
18. Herrera MF, Dominguez AG. Parathyroid embryology, anatomy, and pathology. In: Clark OH, Duh QY, Kebebew E, eds. *Textbook of endocrine surgery*. New Delhi: JP Medical Ltd; 2005:365–371.
19. Irvin GL, Solorzano CC, Carneiro DM. Quick intraoperative parathyroid hormone assay: surgical adjunct to allow limited parathyroidectomy, improve success rate, and predict outcome. *World J Surg*. 2004;28:1287–1292.
20. Falco J, Dip F, Quadri P, de la Fuente M, Rosenthal R. Cutting edge in thyroid surgery: autofluorescence of parathyroid glands. *J Am Coll Surg*. 2016;223:374–380.
21. Brown EM, Gamba G, Riccardi D, Lombardi M, Butters R, Kifor O, et al. Cloning and characterization of an extracellular Ca(2+)-sensing receptor from bovine parathyroid. *Nature*. 1993;366:575–580.
22. Brown EM, MacLeod RJ. Extracellular calcium sensing and extracellular calcium signaling. *Physiol Rev*. 2001;81:239–297.
23. Falco J, Dip F, Quadri P, de la Fuente M, Prunello M, Rosenthal RJ. Increased identification of parathyroid glands using near infrared light during thyroid and parathyroid surgery. *Surg Endosc*. 2017;31:3737–3742.